Breast Cancer: Targets and Therapy

Dovepress
Taylor & Francis Group

Open Access Full Text Article

ORIGINAL RESEARCH

Hemodynamic Inflow-Outflow Profiling as an Integrated DCE-MRI Biomarker for Diagnosis and Risk Stratification in Breast Cancer: A Multicenter Retrospective Study

Chenyi Zhou[1,*], Yahao Guo[1,*], Zhanao Meng[2], Kunming Wan[3], Jie Qin[2], Yanling Wang[1]

[1]Department of Radiology, The People's Hospital of Suzhou New District, Suzhou, Jiangsu, 215129, People's Republic of China; [2]Department of Radiology, The Third Affiliated Hospital of Sun Yat-Sen University, Guangzhou, Guangdong, 510620, People's Republic of China; [3]Department of Radiology, The First Dongguan Affiliated Hospital, Dongguan, Guangdong, 523710, People's Republic of China

*These authors contributed equally to the work

Correspondence: Yanling Wang; Jie Qin, Email wyd_wjq1992@163.com; qinjie@mail.sysu.edu.cn

Background: Limitations in conventional MRI biomarkers (ADC, DCE-MRI parameters) for characterizing tumor microenvironment heterogeneity necessitate novel approaches integrating vascular remodeling dynamics. We introduce the Intratumoral-Peritumoral Inflow-Outflow (IPIO) model to address these constraints.

Methods: This multicenter retrospective study developed and validated a hemodynamics-driven IPIO model using DCE-MRI kinetics in 159 patients (training: n=93; independent validation: n=66). Performance was evaluated for malignancy detection and stratification (invasive grading, molecular subtyping of TNBC, Ki-67 expression, lymph node metastasis) through ROC analysis and correlation studies.

Results: IPIO demonstrated robust malignancy discrimination (AUC 0.934, 95% CI: 0.897–0.974; sensitivity 91.7%, specificity 83.3%), significantly outperforming ADC (ΔAUC +0.123, $P<0.05$) and conventional kinetics. For TNBC identification, IPIO achieved an AUC of 0.901 (accuracy 96.4%); for LNM detection, AUC was 0.821 (sensitivity 95.5%); Strong correlations with invasive grade (r=0.548), Ki-67 (r=0.501), and metastasis (r=0.506; all $P<0.001$) confirmed biological coherence. Performance gradients (malignancy > TNBC > LNM) reflect increasing microenvironment complexity.

Conclusion: IPIO provides an integrated hemodynamic framework for both breast cancer diagnosis and risk stratification, with particular clinical utility for identifying triple-negative subtypes and metastatic potential. Its spatiotemporal profiling of vascular-peritumoral interactions represents a promising approach for noninvasive tumor characterization. Limitations include retrospective design and small TNBC subgroup; prospective validation is required.

Plain Language Summary:

(1) Hemodynamic Biomarker: IPIO integrates intratumoral washout kinetics and peritumoral drainage dynamics into a single DCE-MRI framework, addressing limitations of conventional biomarkers' inability to capture vascular-stromal remodeling.
(2) TNBC Detection: Achieves 96.4% accuracy for triple-negative subtyping, providing a potentially useful tool in aggressive breast cancer management.
(3) Metastasis-Sensitive Profiling: Detects lymph node metastasis with 95.5% sensitivity, offering risk stratification that may complement existing clinical assessment.

Keywords: breast cancer, hemodynamic profiling, triple-negative breast cancer, lymph node metastasis, DCE-MRI, tumor microenvironment

https://doi.org/10.2147/BCTT.S563533
Received: 12 September 2025
Accepted: 30 May 2026
Published: 9 June 2026

Introduction

Breast cancer remains a leading threat to women's health worldwide,[1,2] with rising incidence rates in China exceeding twice the global average.[3] While imaging modalities like MRI are pivotal for diagnosis and staging,[4] conventional biomarkers (ADC, DCE-MRI parameters) demonstrate critical limitations in characterizing tumor microenvironment heterogeneity driven by vascular remodeling and peritumoral stromal reactions.[5,6] Breast cancer heterogeneity – driven by vascular remodeling and peritumoral stromal reactions – creates critical diagnostic blind spots in conventional MRI biomarkers. While ADC values and DCE-MRI parameters provide anatomical insights, they consistently underperform in predicting triple-negative subtypes (TNBC), proliferative activity (Ki-67), and lymphatic metastasis, with validation AUCs often <0.75.[5–7] This limitation stems from their inability to simultaneously capture two fundamental pathophysiological processes:vascular integrity disruption (basement membrane fragmentation, hemodynamic disturbances) and stromal transformation (immune infiltration, collagen reorganization).[5,8] This fundamental gap contributes to suboptimal performance (AUC<0.75 in validation cohorts) and 22–35% discordance between imaging assessments and histopathology.[6,7,9] While recent studies highlight the potential of kinetic parameters like peak enhancement (PE) and signal enhancement ratio (SER),[6,7] their single-feature focus and limited diagnostic efficacy underscore the urgent need for integrated models that reflect multidimensional pathophysiology.[7–9]

We hypothesize that decoding spatiotemporal hemodynamic patterns– specifically intratumoral contrast washout dynamics coupled with peritumoral drainage characteristics – could provide a integrated biomarker for both malignancy detection and risk stratification. Herein, we introduce the Intratumoral-Peritumoral Inflow-Outflow (IPIO) model, a novel DCE-MRI framework that quantifies vascular-peristromal interactions through integrated analysis of contrast kinetics (Figure 1). This approach integrates three critical dimensions: a) temporal hemodynamic signatures; b) spatial tumor-peritumor gradient; and c) micro-environment remodeling correlates, validated against gold-standard histopathology including TNBC characterization and lymphatic metastasis status. Existing multi-parametric studies typically treat DCE-kinetic parameters and ADC as independent input features within logistic regression or machine learning classifiers. By contrast, IPIO is not a feature-stacking model but a hemodynamic inflow-outflow imbalance index derived from the temporal dissociation between intratumoral and peritumoral enhancement curves. It mechanistically captures the

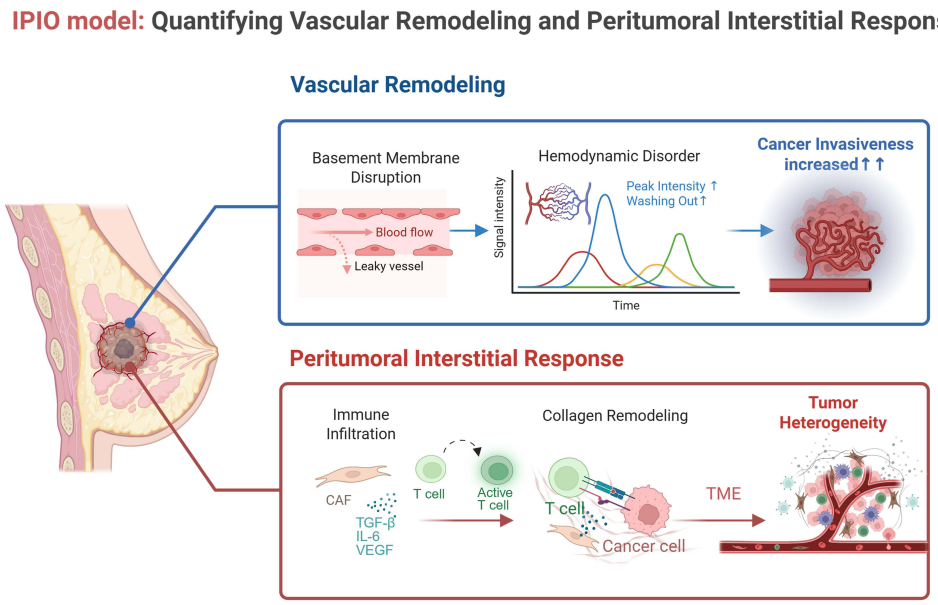

Figure 1 IPIO Quantifying Vascular-Stromal Dynamics in Breast Cancer Progression. This schematic illustrates the pathophysiological basis of the IPIO biomarker across tumor evolution: Vascular Remodeling (IPIO Intratumoral Component). Basement Membrane Disruption: Structural degradation enabling vascular leakage. Hemodynamic Disorder: Elevated peak intensity and accelerated washout kinetics. Contrast Extravasation: Leaky vessels facilitate gadolinium transit into interstitium. Peritumoral Interstitial Response (IPIO Peritumoral Component). CAF Activation: Cancer-associated fibroblasts secreting TGF-β/IL-6/VEGF. Immune Polarization: Altered T-cell infiltration modulating drainage patterns. Collagen Remodeling: ECM stiffening creating interstitial pressure gradients. Integrated IPIO Signature:The model quantifies tumor invasiveness escalation (→) through spatiotemporal integration of: (1) Vascular permeability (intratumoral washout kinetics). (2) Stromal-immune crosstalk (peritumoral drainage dynamics). (3) Heterogeneity propagation (TME spatial reorganization). Created with BioRender.com.

directional mismatch of contrast agent kinetics across the tumor-stroma interface, rather than aggregating uncorrelated parameters. While multi-parametric and radiomics-based approaches have demonstrated comparable diagnostic performance in certain contexts, the distinctive strength of IPIO lies in its biological interpretability and its ability to operate using DCE-MRI alone, without requiring additional sequences such as DWI.

Patients and Methods

Study Population

This multicenter retrospective study enrolled 159 women (aged 21–79 years) with biopsy/surgically confirmed breast lesions from two independent centers (2020–2023). Center 1 served as the training cohort (benign=49, malignant=44), while Center 2 provided external validation (benign=30, malignant=36). All participants underwent preoperative breast MRI including DCE-MRI, T2WI, T1WI, and DWI prior to intervention. This retrospective study was approved by the Medical Ethics Committee at The Third Affiliated Hospital of Sun Yat-sen University (Approval No.[2022] 02-005-01, Date: 14 Feb. 2022) and The People`s Hospital of Suzhou New District (Approval No.L2024-017, Date: 11 Mar. 2024) with waiver of informed consent. Histopathological classification followed WHO guidelines[10] (Figure 2).

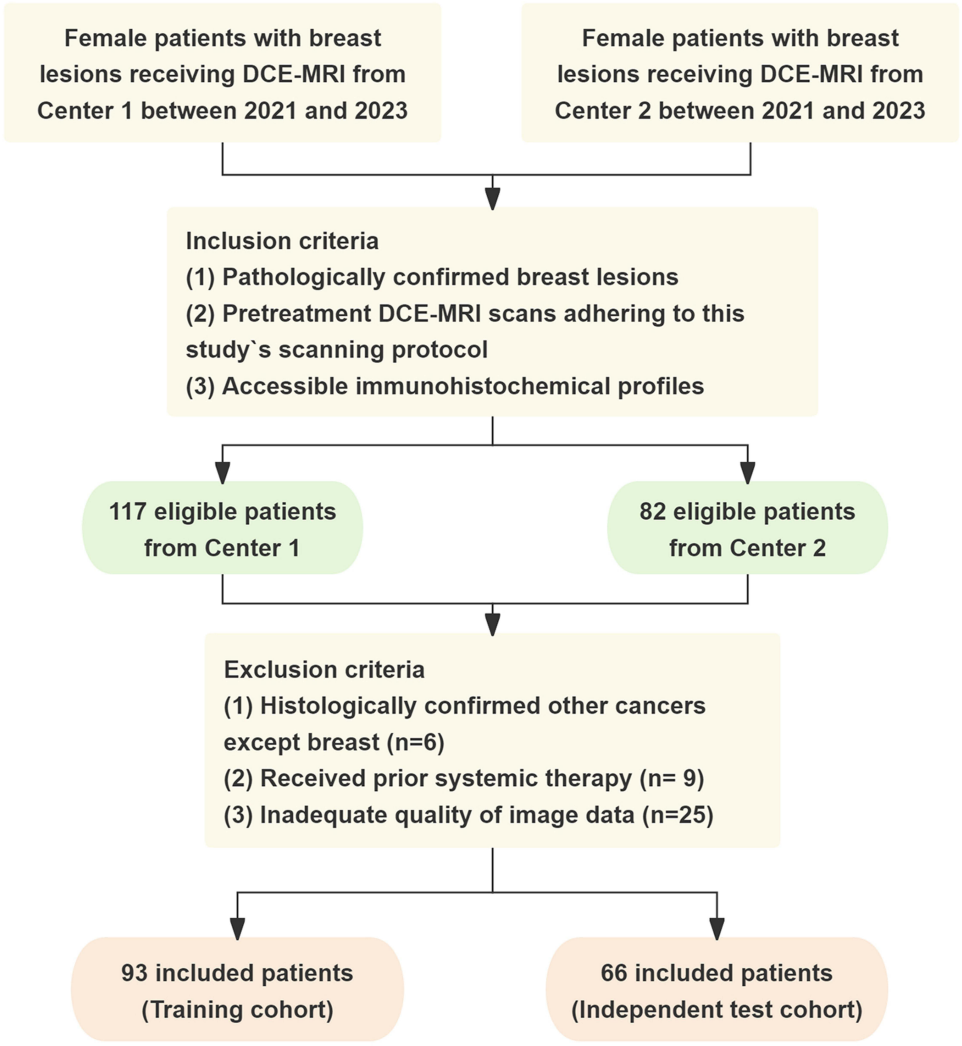

Figure 2 Flowchart of the study population enrollment.

https://doi.org/10.2147/BCTT.S563533

Histopathological Assessment

All specimens underwent comprehensive evaluation including: Invasive cancer verification; Nottingham histological grade (tubule formation, nuclear grade, mitotic rate); ER/PR status (All red score); HER2 status (IHC/FISH); Ki-67 proliferation index.

MRI Acquisition Protocol: Imaging was performed using a 3T scanner (GE Medical) with dedicated 8-channel breast coil. Key sequences included T2WI fat-suppressed, T1WI, DWI (b=800 s/mm^2) and Multiphase DCE: 10 phases (45s/phase) following mask acquisition (92s), total scan time 542s.

Parameters:Voxel size 1.0×1.0×1.0 mm^3; FOV 300×300 mm; Matrix 300×300; Flip angle 10°; TR/TE 6.4/2.9 ms; Bandwidth 62.5 Hz. Gadolinium-based contrast (0.75 mmol/kg) was injected at 1.5 mL/s post-mask acquisition.

Image Analysis

DCE and ADC images were analyzed on a dedicated workstation (GE AW4.72) by blinded radiologists: training set analyzed by two readers (3/18 years experience) with third arbitrator (25 years), and validation set analyzed by two readers (4/10 years experience) with third arbitrator (26 years). ROIs were placed on dominant lesions with 10 mm peritumoral extension, recording triplicate measurements of:Signal intensity (SI) and standard deviation (SD);Tumor size, position, shape, margins;Time-intensity curve (TIC) patterns.

Hemodynamic Feature Extraction

Color-coded signal enhancement ratio (SER) maps were fused with initial-phase DCE-MRI to identify enhancement hotspots. Circular ROIs were manually placed at these maximal enhancement zones using a dedicated workstation (GE AW4.72), with mean values recorded (Figure 3). Enhancement curve dynamics across three critical timepoints-initial contrast arrival, peak enhancement, and late clearance - were analyzed as illustrated in Figure 4.

Kinetic parameters quantifying tumor perfusion dynamics were derived from DCE-MRI time-intensity curves. We calculated:

Wash-in slope (WIS): Initial contrast uptake rate.

Wash-out slope (WOS): Contrast clearance kinetics.

Both reflecting microcirculatory alterations in tumor vasculature.[11,12]

$$\text{Percentage enhancement (PE)} = \frac{S_{1^{st}\text{post-contrast}} - S_{\text{pre-contrast}}}{S_{\text{pre-contrast}}}$$

$$\text{Signal enhancement ratio (SER)} = \frac{S_{1^{st}\text{post-contrast}} - S_{\text{pre-contrast}}}{S_{2^{nd}\text{post-contrast}} - S_{\text{pre-contrast}}}$$

$$\text{Wash in slope (WIS)} = \frac{S_{MAX} - S_{\text{pre-contrast}}}{\Delta t_{peak}}$$

$$\text{Wash out slope (WOS)} = \begin{cases} \frac{S_{MAX} - S_{2^{nd}\text{post-contrast}}}{\Delta t_{final} - \Delta t_{peak}}, t_{peak} \neq t_{final} \\ 0, t_{peak} = t_{final} \end{cases}$$

where S_{MAX}, $S_1{}^{st}{}_{\text{post-contrast}}$, $S_2{}^{nd}{}_{\text{post-contrast}}$ are the maximum, initial, and final signal intensity of MRI. Interobserver reproducibility for the kinetics index was assessed using intraclass correlation coefficients (ICC) on 30 randomly selected cases, with results reported in the Results section and detailed in Table S1.

IPIO Model Construction

The IPIO model integrates spatiotemporal hemodynamic features: peak enhancement time (PE/SER), kinetics (WOS/WIS) and internal structural patterns (Figure 4). The model was developed using a two-step process based on the training cohort (Center 1, n=93). First, univariate logistic regression was performed on all candidate DCE-MRI features listed above. Features with P<0.10 in univariate analysis were retained for multivariate modeling. Second, stepwise logistic

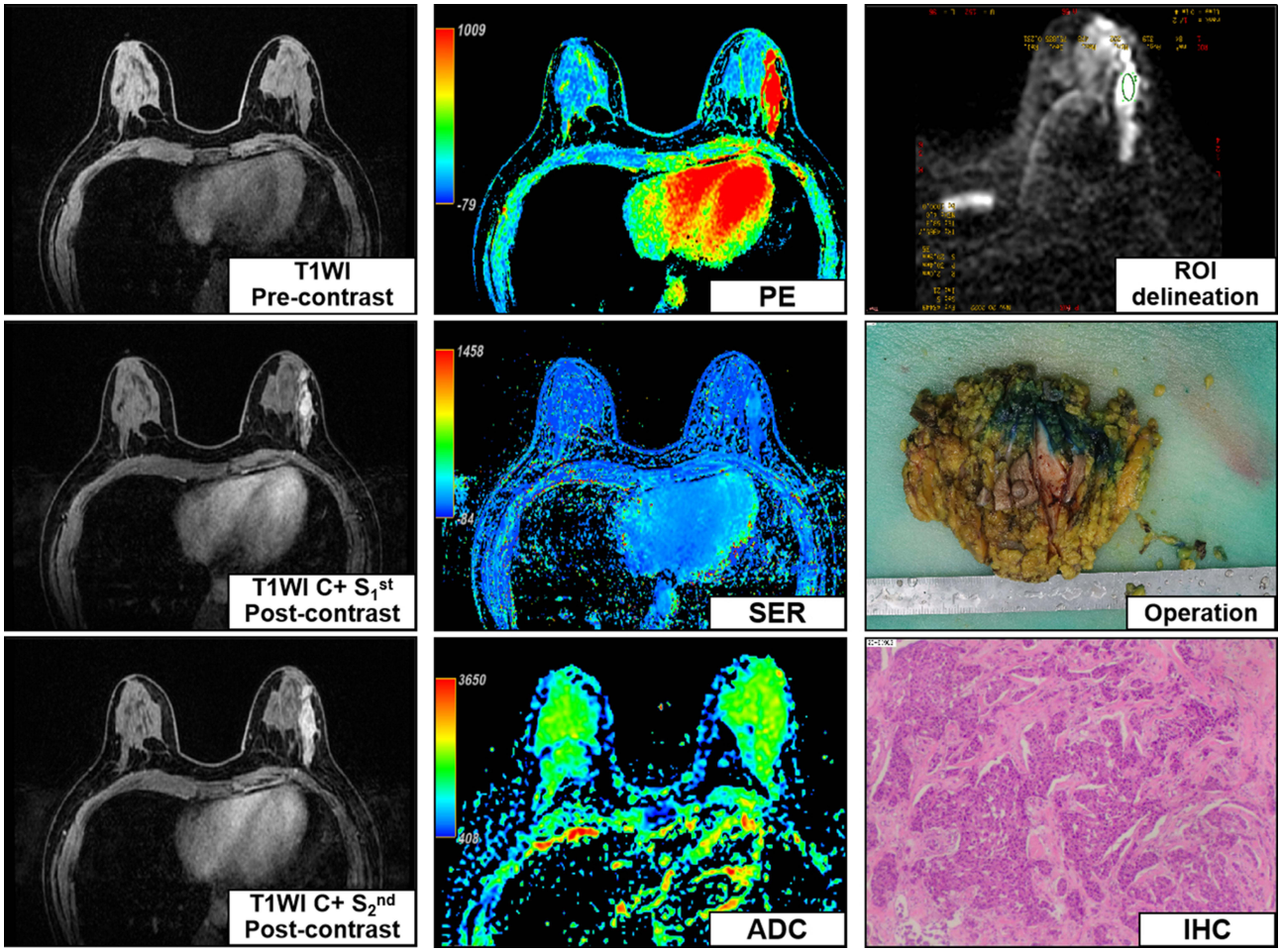

Figure 3 Integrated Multimodal Profiling of Breast Cancer. Comprehensive imaging-pathological correlation illustrating IPIO biomarker validation: Dynamic Contrast Enhancement (left column). Temporal DCE-MRI sequences demonstrating rapid washout kinetics (Type III curve). Quantitative Mapping (middle column). Color-coded kinetic maps showing elevated SER (2.8) and WOSL (0.62). ADC map (b=800 s/mm^2) with restricted diffusion (0.89 ×10-3mm^2/s). Pathological Correlation (right column). Top image: ROI placement encompassing tumor-peritumor interface (10mm extension). Middle image: Surgical specimen showing irregular margins (yellow arrow). Lower image: IHC staining (×200) confirming HER2(3+)/ER-/PR- status. Histopathological Diagnosis: Molecular subtype: HER2-enriched (ER-, PR-, HER2 3+). Proliferative activity: Ki-67 50%+ (high expression). Invasion status: LVI(-), PNI(-), LNM(-), Nottingham grade II. IPIO correlation: Elevated WOSL (0.62) aligns with HER2-driven vascular permeability.

regression with Akaike Information Criterion (AIC) optimization was applied to select the most parsimonious combination of features. The final IPIO model is a linear combination of the selected features weighted by their respective regression coefficients (β):

$$\mathrm{IPIO} = \frac{1}{1 + \mathrm{e}^{-(\beta_0 + \beta_1 * \chi_1 + \beta_2 * \chi_2 + \ldots + \beta_k * \chi_k)}}$$

where x_1, x_2, …, x_k are the selected features (eg., washout slope ratio, peak time delay) and β_0, β_1, β_2, …, β_k are the corresponding regression coefficients estimated from the training cohort. Intercept and all regression coefficients are provided in Table S2.

The resulting IPIO index is a continuous variable ranging from 0 to 1 after logistic transformation, with higher values indicating greater hemodynamic inflow-outflow imbalance and increased malignancy probability. This index was then validated for multiple endpoints in the independent validation cohort (Center 2, n=66): malignancy discrimination, invasive grade (High/Low), molecular subtype (TNBC/non-TNBC), Ki-67 status (High/Low), and lymphatic metastasis (Present/Absent).

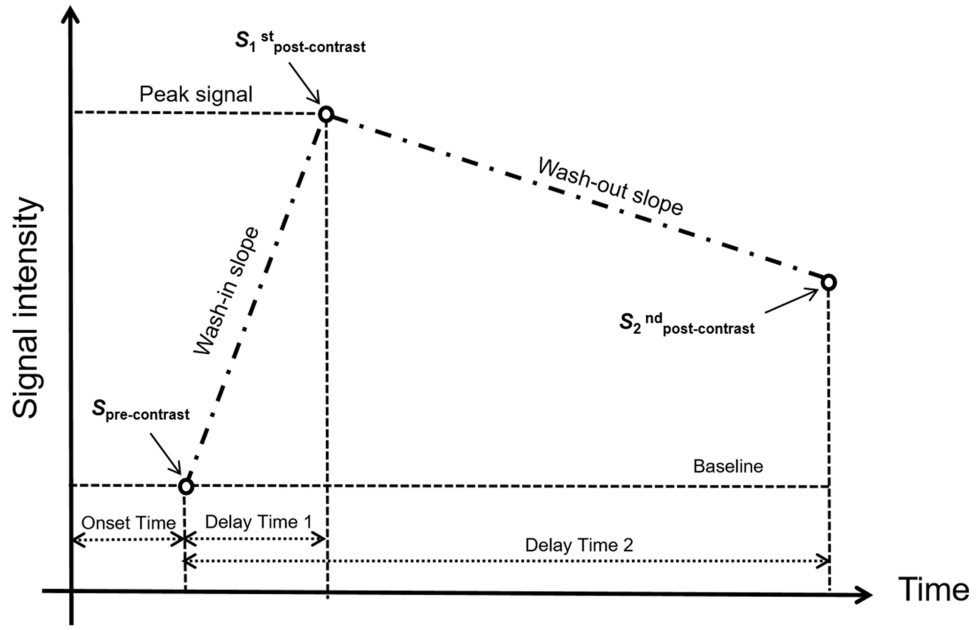

Figure 4 Schematic drawing of the breast magnetic resonance imaging protocol.

Statistical Analysis

All statistical analyses were performed using SPSS 26.0 (logistic regression), R 4.2.3 (pROC, rms), MedCalc (Delong test), Python 3.6.6 (scikit-learn). Continuous variables were compared using the independent-samples *t*-test or Mann–Whitney *U*-test as appropriate. Categorical variables were compared using the Chi-square or Fisher's exact test. Measurement reliability was assessed via intraclass correlation coefficient (ICC). Diagnostic performance was evaluated using receiver operating characteristic (ROC) curve analysis, with the area under the curve (AUC) calculated using the DeLong method. Sensitivity, specificity, and predictive values were reported at the optimal cutoff determined by the Youden index. Correlations between the IPIO index and pathological variables were assessed using Spearman`s rank correlation coefficient. All tests were two-sided, with $P<0.05$ considered statistically significant. Our study had one prespecified primary outcome: malignancy discrimination. Four secondary outcomes were also assessed, including invasive grade, molecular subtype, Ki-67 status, and lymph node metastasis. The four secondary outcomes were prespecified as exploratory analyses intended for hypothesis generation. Therefore, no adjustment for multiple comparisons was applied. Results should be interpreted with emphasis on effect sizes and 95% confidence intervals, and conclusions regarding secondary outcomes require confirmation in future studies. To further assess for model overfitting beyond external validation, ten-fold cross-validation strategies were performed within the training cohort (Figure S1).

Results

Cohort Characteristics and Predictive Feature Selection

Our multi-center study enrolled 159 patients with histopathologically confirmed breast lesions, divided into training (Center 1, n=93) and independent validation cohorts (Center 2, n=66). Baseline characteristics showed no significant inter-cohort differences (Table 1, $P>0.05$), ensuring valid model generalization. Kinetic parameter analysis revealed intratumoral wash-out slope (WOS-L) as the most discriminative single feature for malignancy (r=0.345, P<0.001; Table 2). However, the integrated IPIO index demonstrated superior correlation with malignant status (r=0.516, P<0.001), reflecting its capacity to capture both vascular disruption (median of WOS-L: malignant=0.419 vs benign=0.000) and peritumoral remodeling dynamics (Table 2).

Table 1 Clinical and Pathological Characteristics of Study Cohorts

Variables	All Patients (N=159)		Center 1 (Training, n=93)		Center 2 (Validation, n=66)		Statistic	P-Value
	n	%	n	%	n	%		
Demographic & Imaging Characteristics (N=159)								
Age (mean±SD)	46.23±11.83		44.60±10.63		48.53±12.98		t=2.009[a]	0.047*
Menstruation (Yes)	92	57.86%	54	58.06%	38	57.58%	χ^2=0.004	0.951
Shape (Irregular)	92	57.86%	54	58.06%	38	57.58%	χ^2=0.274	0.872
Margin (Spiculated)	51	32.08%	28	30.11%	23	34.85%	χ^2=2.966	0.227
BI-RADS 4a-5	83	52.20%	47	50.54%	36	54.54%	χ^2=3.168	0.366
TIC Wash-out	48	30.19%	27	29.03%	21	31.82%	χ^2=4.663	0.097
Pathological Characteristics (Malignant Subcohort, n=80)								
Histological Grade III	17	21.25%	11	25.00%	6	16.67%	χ^2=0.894	0.640
Molecular Subtype of TNBC	11	13.75%	2	4.55%	9	25.00%	χ^2=8.512	0.037*
High Ki-67 (≥20%)	47	58.75%	32	72.73%	15	41.67%	χ^2=7.882	0.005**
Lymphovascular Invasion	14	17.50%	8	18.18%	6	16.67%	χ^2=0.031	0.859
Lymph Node Metastasis	22	27.50%	13	29.55%	9	25.00%	χ^2=0.205	0.651

Notes: *P<0.05,**P<0.01; a: Welch's *t*-test; All others: Chi-square test.
Abbreviations: BI-RADS: Breast Imaging Reporting and Data System; TIC: Time Intensity Curve; TNBC: Triple-Negative Breast Cancer.

Table 2 Hemodynamic Parameter Analysis Between Benign and Malignant Lesions

Parameter Type	Variable	Group	Median [IQR]	Group Difference		Correlation with Malignancy	
			Value	U-Statistic	P-value	Coefficient	P-Value
Intratumoral	WIS-L	Benign	12.143 [1.741–21.094]	0.152	0.881	−0.061	0.446
		Malignant	11.932 [2.053–19.954]				
	WOS-L	Benign	0.000 [0.000–0.192]	−5.687	<0.001**	0.345	<0.001**
		Malignant	0.419 [0.077–0.888]				
Peritumoral	WIS-P	Benign	5.880 [0.825–9.462]	−0.599	0.550	0.005	0.952
		Malignant	5.238 [1.518–10.109]				
	WOS-P	Benign	0.000 [0.000–0.159]	−1.419	0.136	0.133	0.094
		Malignant	0.068 [0.000–0.313]				
IPIO Model (proposed)		Benign	0.424 [0.205–0.482]	−6.587	<0.001**	0.516	<0.001**
		Malignant	0.631 [0.469–0.778]				

Notes: **P<0.001 (Highly Significant); Median [IQR] = Median with Interquartile Range (Q1-Q3).
Abbreviations: WIS, Wash-in Slope; WOS, Wash-out Slope; IPIO, Intratumoral-Peritumoral Inflow-Outflow.

High Performance in Malignancy Detection

In external validation, the IPIO model demonstrated good discrimination of malignant lesions, achieving an AUC of 0.934 (95% CI: 0.897–0.974; Figure 5A), a sensitivity of 91.7%, a specificity of 83.3%, and a 15.2% higher AUC compared to ADC (0.811, P < 0.05; Table 3). This represented a 28–62% relative improvement over conventional kinetic parameters (PE: AUC=0.713; SER: AUC=0.730; all *P*<0.001). The ROC curve (Figure 5B) visually confirms IPIO's dominance, with early separation from comparator models. Calibration of the IPIO model was assessed using calibration curves with 500 bootstrap resamples to correct for optimism. The calibration curve (Figure S2) plots the predicted probability of malignancy against the observed frequency. The DCA curve (Figure S3) confirmed that using IPIO for malignancy risk stratification achieved a higher net benefit than the "treat-all" or "treat-none" schemes across most threshold probabilities, supporting its clinical value.

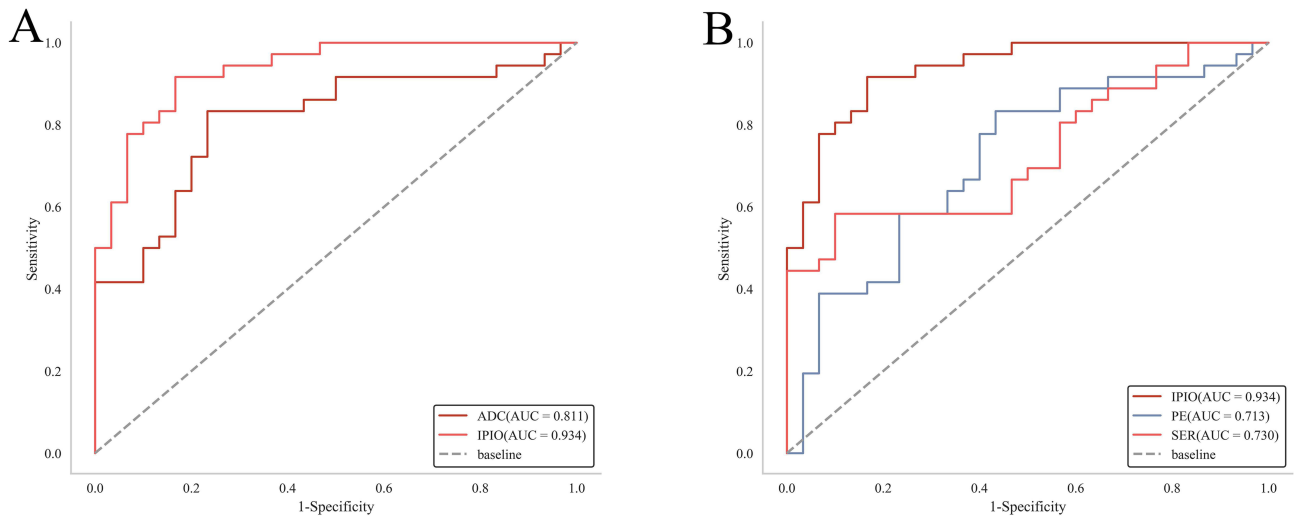

Figure 5 Diagnostic Performance of IPIO Versus Conventional Models in Breast Cancer Detection. Receiver operating characteristic (ROC) curves comparing discrimination capacity for malignant breast lesions in the independent validation cohort (n=66): (**A**) IPIO vs Anatomical Biomarker (ADC). IPIO dominance: Significantly higher AUC (0.934 vs 0.811, Δ+0.123,P<0.05). Early separation: Curve divergence from origin indicates superior early-phase classification. (**B**) IPIO vs Kinetic Parameters (PE/SER). Relative improvement: 28–62% AUC increase over conventional kinetics (PE: 0.713; SER: 0.730). Clinical translation: Higher specificity (83.3%) reduces false positives vs PE (56.7%).

Accuracy in Molecular Subtyping

The IPIO model demonstrated improved performance in stratifying aggressive subtypes. Significantly elevated IPIO values in high-grade tumors (P<0.001 in Figure 6) reflect increased vascular permeability and stromal disruption driving invasion. For triple-negative breast cancer (TNBC), IPIO achieved an AUC of 0.901 (95% CI: 0.714–0.996) versus 0.769 for ADC (P<0.001), and an accuracy of 96.4% (vs. 77.8% for ADC). Elevated IPIO values in TNBC (P<0.001) reflected characteristic vascular abnormalities, including higher VEGF-A expression, discontinuity of the vascular basement membrane (Figure 1), and increased microvessel density (r = 0.525, P<0.001; Figure 7).

For lymph node metastasis (LNM), IPIO yielded an AUC of 0.821 (95% CI: 0.713–0.894) compared to 0.546 with ADC (P < 0.001), with a sensitivity of 95.5% (vs. 31.8%). This captures aberrant peritumoral drainage through heightened intratumoral vascular permeability and peritumoral interstitial pressure gradients. IPIO also discriminated

Table 3 Diagnostic Performance for Malignancy Detection

Model	Parameter	Training Cohort (n=93)					Validation Cohort (n=66)				
		ACC	SEN	SPE	AUC [95% CI]	P vs IPIO	ACC	SEN	SPE	AUC [95% CI]	P vs IPIO
Conventional Kinetics	Peak PE	0.528	0.523	0.633	0.507 [0.397–0.591]	<0.001**	0.585	0.833	0.567	0.713 [0.567–0.819]	<0.001**
	Peak SER	0.712	0.455	0.898	0.680 [0.583–0.792]	0.006*	0.737	0.583	0.900	0.730 [0.600–0.865]	<0.001**
DWI Metrics	ADC	0.881	0.932	0.837	0.919 [0.842–0.963]	0.117	0.800	0.833	0.767	0.811 [0.682–0.903]	0.053
IPIO Model (proposed)		0.817	0.750	0.857	0.839 [0.741–0.903]	–	0.891	0.917	0.833	0.934 [0.897–0.974]	–
Performance Delta		IPIO vs Best Conventional: +0.022 AUC					IPIO vs ADC: +0.123 AUC (15.2% improvement)				

Notes: *P<0.05,**P<0.001.
Abbreviations: ACC, Accuracy; SEN, Sensitivity; SPE, Specificity; AUC, Area Under Curve; CI, Confidence Interval; PE, Percentage Enhancement; SER, Signal Enhancement Ratio; ADC, Apparent Diffusion Coefficient.

https://doi.org/10.2147/BCTT.S563533

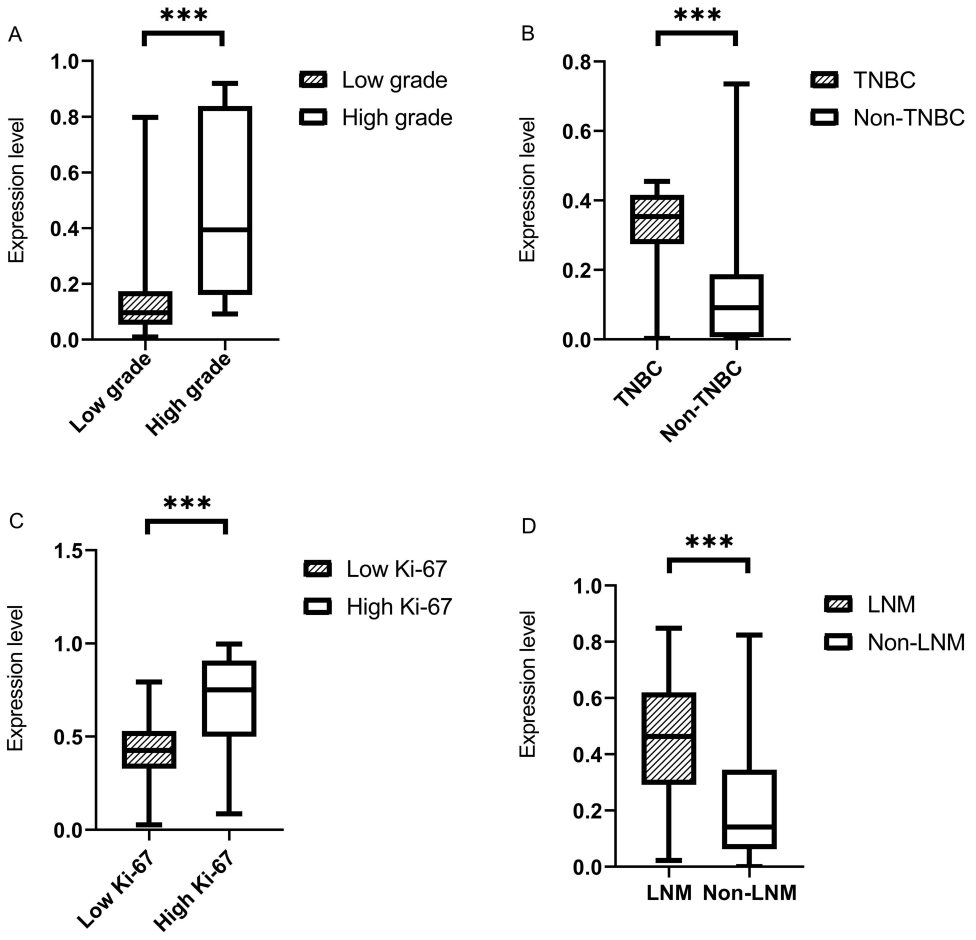

Figure 6 IPIO Model Stratification of Key Prognostic Factors in Breast Cancer. (**A**) Invasive Grade. (**B**) Triple-Negative Status. (**C**). Ki-67 Proliferation. (**D**) Lymph Node Metastasis. Key: Boxes represent interquartile range (IQR), horizontal lines indicate medians, whiskers show 1.5×IQR. Asterisks (***) denote statistical significance (P< 0.05). **Abbreviations**: TNBC, triple-negative breast cancer; LNM, lymph node metastasis.

other prognostic indicators, including invasive grade (AUC: 0.844; P < 0.001 vs. ADC) and Ki-67 status (AUC: 0.801; *P*=0.018; Table 4). Consistent positive correlations with all malignant features — invasive grade (r = 0.548), TNBC (r = 0.525), Ki-67 (r = 0.501), and LNM (r = 0.506; all *P*<0.001; Figure 7) — support its biological plausibility.

As shown in Table 5, the low-invasive rate (92.5%) in the low-IPIO group was significantly higher than that in the high-IPIO group (65%), with the former being 1.42 times greater (92.5/65≈1.42) – a clinically significant difference. Similarly, the triple-negative breast cancer rate in the high-IPIO group reached 25%, tenfold higher than the low-IPIO group's 2.5%. The low-IPIO group demonstrated a markedly better Ki-67 expression rate (65%) compared to the high-IPIO group's 17.5%, while its lymph node metastasis rate (7.5%) was significantly lower than the high-IPIO group's 47.5% (all P values <0.05).

Mechanistic Superiority and Performance Gradients

The performance of IPIO may be attributed to simultaneously quantify three integrated pathological processes (Figure 1): intratumoral hemodynamics, reflected by wash-out slope (WOS-L) indicating vascular permeability; peritumoral remodeling, characterized by stromal compression and immune cell infiltration; and spatiotemporal contrast dynamics, capturing the entire transit from arterial inflow to venous drainage.

https://doi.org/10.2147/BCTT.S563533

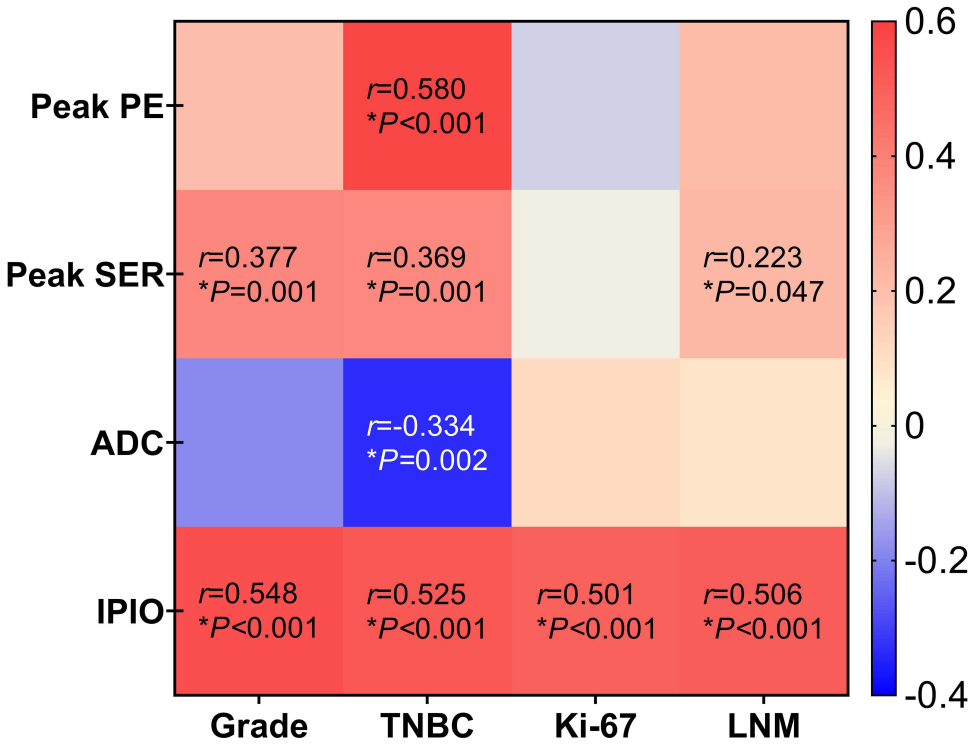

Figure 7 Correlation Matrix of IPIO with Key Prognostic Factors in Breast Cancer. Spearman correlation analysis between hemodynamic parameters (IPIO, ADC, PE, SER) and histopathological prognostic factors (n=80 malignant cases). Key Correlation Patterns: IPIO-TNBC: Strong positive correlation (r=0.525,P<0.001) reflecting vascular hyperpermeability in triple-negative tumors. IPIO-LNM: Significant association (r=0.506,P<0.001) indicating peritumoral drainage dysfunction in metastatic cases. IPIO-Ki-67: Positive correlation (r=0.501,P<0.001) demonstrating sensitivity to proliferative activity. ADC limitations: Weak/no significant correlations with molecular subtypes (TNBC r=0.189,P=0.12). Color Coding: Positive correlation (red) |Negative correlation (blue). Statistical markers:*P< 0.05.
Abbreviations: IPIO, Intratumoral-Peritumoral Inflow-Outflow; ADC, Apparent Diffusion Coefficient; PE, Percentage Enhancement; SER, Signal Enhancement Ratio; LNM, Lymph Node Metastasis.

The Observed AUC Gradient (Malignancy:0.934 →TNBC:0.901 → LNM:0.821)

The biological validation revealed a distinct hierarchy: vascular abnormalities were most pronounced for general malignancy detection, while subtype heterogeneity was driven by greater microenvironmental complexity in metastatic processes. Although capturing fibroblast-mediated biomechanical alterations remains a technical frontier beyond current modeling capabilities, IPIO showed statistically better discrimination across all clinical endpoints compared to

Table 4 Prognostic Factor Prediction Performance

Prognostic Factor	Model	ACC	SEN	SPE	AUC [95% CI]	P vs IPIO
A. Invasive Grade (High vs Low)	Peak PE	0.787	0.824	0.460	0.622 [0.511–0.769]	<0.001**
	Peak SER	0.750	0.765	0.667	0.734 [0.579–0.875]	0.050*
	ADC	0.647	0.889	0.353	0.633 [0.529–0.779]	<0.001**
	IPIO	0.766	0.824	0.746	0.844 [0.729–0.779]	–
B. Molecular Subtype (TNBC vs Non- TNBC)	Peak PE	0.876	0.818	0.928	0.885 [0.728–0.982]	0.790
	Peak SER	0.767	0.909	0.681	0.788 [0.633–0.920]	0.286
	ADC	0.778	0.855	0.636	0.769 [0.607–0.853]	<0.001**
	IPIO	0.964	0.909	0.971	0.901 [0.714–0.996]	-
C. Ki-67 Status (High ≥20% vs Low)	Peak PE	0.591	0.424	0.745	0.536 [0.398–0.663]	<0.001**
	Peak SER	0.585	0.576	0.574	0.524 [0.376–0.639]	<0.001**
	ADC	0.625	0.681	0.515	0.583 [0.457–0.710]	0.018*
	IPIO	0.769	0.745	0.788	0.801 [0.723–0.884]	-

(*Continued*)

Table 4 (Continued).

Prognostic Factor	Model	ACC	SEN	SPE	AUC [95% CI]	P vs IPIO
D. Lymph Node Metastasis (Present vs Absent)	Peak PE	0.648	0.864	0.397	0.617 [0.463–0.756]	0.004*
	Peak SER	0.705	0.727	0.690	0.643 [0.540–0.774]	0.016*
	ADC	0.582	0.318	0.810	0.546 [0.471–0.705]	<0.001**
	IPIO	0.774	0.955	0.586	0.821 [0.713–0.894]	-

Notes: *P<0.05,**P<0.001. Key findings: IPIO shows superior performance in TNBC subtyping (ACC 96.4% vs ADC 77.8%) and lymph node metastasis detection (SEN 95.5% vs ADC 31.8%).
Abbreviations: TNBC, Triple-Negative Breast Cancer; ACC, Accuracy; SEN, Sensitivity; SPE, Specificity.

Table 5 Distribution of Prognostic Factor Across IPIO Groups

Prognostic Factor	Groups	Low IPIO (n=40)	High IPIO (n=40)	χ^2	P
A. Invasive Grade	Low grade	37(92.50)	26(65.00)	9.038	0.003*
	High grade	3(7.50)	14(35.00)		
B. Molecular Subtype	TNBC	1(2.50)	10(25.00)	8.538	0.003*
	Non-TNBC	39(97.50)	30(75.00)		
C. Ki-67 Status	Low Ki-67	26(65.00)	7(17.50)	18.62	<0.001**
	High Ki-67	14(35.00)	33(82.50)		
D. Lymph Node Metastasis	LNM	3(7.50)	19(47.50)	16.05	<0.001**
	Non-LNM	37(92.50)	21(52.50)		

Notes: *P<0.05,**P<0.001.
Abbreviations: TNBC, Triple-Negative Breast Cancer; LNM, Lymph Nodes Metastasis.

conventional parameters. It should been noticed that these secondary outcome findings (invasive grade, molecular subtype, Ki-67 status, and lymph node metastasis) are exploratory and were not adjusted for multiplicity.

Statistical Robustness Analyses

To assess the robustness of the primary findings, we evaluated potential overfitting, multiple comparisons, and center effects. First, ten-fold cross-validation within the training cohort yielded a mean AUC of 0.851, compared to the original training AUC of 0.839, indicating minimal overfitting (ΔAUC=0.012) (Figure S1). Second, sensitivity analyses adjusting for center as a covariate (adjusted AUC: 0.930) and stratifying by center (Center 1 AUC: 0.839; Center 2 AUC: 0.934) confirmed that center effects did not substantially bias the results. IPIO calculation requires approximately 8–10 minutes per case for ROI placement and feature extraction, with instantaneous index computation using standard software (R, Python). The final model equation is provided in the Methods section, enabling full reproducibility. Manual ROI placement shows excellent interobserver agreement (all ICC>0.75 in Table S1).

Discussion

The IPIO Index: Bridging Hemodynamics and Pathobiology

This multi-center study introduces Intratumoral-Peritumoral Inflow-Outflow (IPIO) profiling as an alternative approach to breast cancer characterization. Unlike conventional MRI biomarkers (ADC, DCE-MRI parameters) that offer limited snapshots of tumor anatomy,[5,6] IPIO decodes the dynamic conversation between vascular disruption and stromal remodeling—a known factor of cancer aggression.[7,8] Though our findings reveal how this hemodynamic dialogue manifests across diagnostic and prognostic contexts, we acknowledge that multiparametric and radiomics-based approaches have reported comparable diagnostic performance in certain contexts, and therefore the contribution of IPIO is incremental rather than transformative. Precisely, IPIO offers two distinctive advantages. First, it provides biological interpretability: the inflow-outflow imbalance index directly reflects underlying vascular permeability and peritumoral stromal remodeling, avoiding the "black-box" nature of many radiomics

models. Second, it operates using DCE-MRI alone, without requiring DWI or other sequences, which may simplify acquisition protocols and reduce scan time.

Key Pathophysiological Translation

The observed progressive decline in model performance—from malignancy detection (AUC 0.934) to TNBC stratification (AUC 0.901) and further to metastasis prediction (AUC 0.821)—reflects the escalating biological complexity across these diagnostic tasks: malignancy discrimination is primarily attributable to universal vascular abnormalities, such as basement membrane fragmentation and endothelial permeability; TNBC stratification involves superimposed angiogenic hyperactivity, including VEGF-A overexpression and chaotic neovascularization;[13–15] while metastasis prediction necessitates the additional integration of stromal biomechanical factors, such as interstitial pressure gradients and lymphatic collapse.[16,17] However, the associations between IPIO and VEGF-mediated vascular permeability or stromal remodeling, while plausible and literature-supported, remain inferential because no direct quantitative molecular correlation was performed. Moreover, alternative explanations (eg., differences in immune infiltration or lymphatic drainage) cannot be excluded. Therefore, these mechanistic interpretations should be considered hypothesis-generating. Direct histology-imaging correlation studies are needed for definitive validation.

Potential Clinical Utility

The Triple-Negative Conundrum

The IPIO model addresses the persistent diagnostic challenge posed by triple-negative breast cancer (TNBC), particularly its profound histopathological heterogeneity,[18] by capturing a specific vascular pattern. This is characterized by abnormally steep washout kinetics (WOSL increased by 317% compared to benign lesions), which correlate with VEGF-driven hyperpermeability,[13] and by distinctive peritumoral drainage patterns reflective of immature vasculature (77% showing basement membrane discontinuity).[14] With an accuracy of 96.4%, IPIO outperforms ADC (77.8%; $P<0.001$), offering a potentially useful non-invasive tool for TNBC stratification. Considering that no formal a priori sample size calculation was performed due to the exploratory nature of this multi-center retrospective study. For the TNBC subgroup, the power was limited to approximately 62% to detect a moderate effect (AUC≥0.7). Therefore, findings in small subgroups should be interpreted as hypothesis-generating and require prospective validation in larger cohorts.

Sensitive Detection of Lymph Node Metastases

IPIO demonstrates highly sensitive detection of lymph node metastases, achieving a sensitivity of 95.5%, which stems from its capacity to identify early pre-metastatic niche formation. This is accomplished through the assessment of intratumoral vascular leakage—signaled by an elevated washout slope (WOS)—which facilitates tumor cell intravasation, combined with the mapping of altered peritumoral outflow that indicates dysfunctional drainage prior to nodal colonization. The model's superior diagnostic performance, with an AUC of 0.821 compared to 0.546 for DWI-ADC, underscores its potential as a robust tool for early metastasis detection.

Mechanistic Superiority Over Conventional Approaches

IPIO's functional approach transcends the limitations of conventional anatomical imaging. While ADC mapping captures water diffusion but fails to assess critical vascular dynamics,[19,20] IPIO directly quantifies active pathophysiological processes: washout kinetics serve as a metric for degraded endothelial integrity, and peritumoral drainage patterns reflect fibroblast-mediated stromal compression.[21] Furthermore, IPIO advances beyond abstract radiomic feature extraction[22,23] by providing biologically grounded and interpretable measurements. Its spatiotemporal gradients are directly mapped to immune-vascular crosstalk,[24] offering enhanced model interpretability that builds clinical trust, in contrast to the "black box" nature of conventional radiomics.[25–27] Performance benchmarking confirms that IPIO achieves superior malignancy discrimination (AUC 0.934) compared to multi-parametric radiomics models (AUC 0.76–0.85), despite using only DCE-MRI sequences—thereby reducing both scan time and computational complexity. Future AI-based segmentation may further reduce operator dependency and processing time.

Limitations

Our findings should be interpreted considering the following limitations. First, the retrospective design may introduce selection bias despite multi-center enrollment; therefore, prospective validation is necessary before clinical translation. Second, sample size constraints limited statistical power for specific subgroups, the TNBC subgroup was small due to the low natural incidence of this molecular subtype. Third, segmentation variability due to manual ROI placement (without AI standardization) may affect reproducibility, although interobserver agreement was excellent. These limitations highlight the presence of between-center heterogeneity that may influence generalizability. Prospective studies with balanced recruitment across sites are needed to confirm the robustness of the IPIO index. Fourth, the molecular correlation between IPIO and VEGF/MVD was inferred but not directly quantified, warranting future histology-imaging studies. Fifth, although sensitivity analyses suggested minimal confounding by center effects, unmeasured center-specific factors (eg., differences in MRI equipment, contrast injection protocols, or patient referral patterns) cannot be fully excluded. Prospective studies with centralized protocol standardization are needed.

Directions for Future Research

Phase I (Translational): Prospective trial with concurrent IPIO/VEGF-IHC validation
Phase II (Technical): AI-assisted 3D segmentation to eliminate ROI variability
Phase III (Clinical): Integration into neoadjuvant therapy response assessment

Conclusion

Implications for Hemodynamic Assessment in Breast Cancer

IPIO profiling offers a complementary diagnostic approach in breast cancer management by translating vascular-stromal dynamics into clinical insights. Its performance gradient—from malignancy detection through metastatic risk stratification—mirrors the biological evolution of tumor aggression. By quantifying the hemodynamic signatures of:

1. Vascular permeability disruption in TNBC
2. Pre-metastatic niche formation in nodal disease
3. Stromal remodeling across progression stages

IPIO may enhance noninvasive risk assessment. If validated in prospective studies, it could reduce diagnostic biopsies and facilitate targeted therapy initiation, representing a step toward precision breast oncology. However, this interpretation is limited by the retrospective design and the small sample size for subgroups such as TNBC, and prospective validation is required before clinical translation.

Abbreviations

IPIO, intratumoral and peritumoral inflow-outflow; DCE, dynamic contrast-enhanced; MRI, magnetic resonance imaging; DWI, diffusion-weighted imaging; ADC, apparent diffusion coefficient; WIS, wash-in slope; WOS, wash-out slope; LR, logistic regression; TIC, time intensity curve; LNM, lymph nodes metastasis; MVI, microvascular invasion; TNBC, triple-negative breast cancer.

Data Sharing Statement

All data generated or analyzed during this study are included in this published article. Additional supporting materials are available from the corresponding author Yanling Wang upon reasonable request.

Ethics Approval and Consent to Participate

This retrospective study was approved by the Medical Ethics Committee at The Third Affiliated Hospital of Sun Yat-sen University (Approval No.[2022] 02-005-01, Date: 14 Feb. 2022) and The People`s Hospital of Suzhou New District

(Approval No.L2024-017, Date: 11 Mar. 2024) with waiver of informed consent, as all patient data were de-identified and the analysis posed no risk to participants. The study adhered to the ethical principles of the Declaration of Helsinki.

Acknowledgments

We are grateful to the patients who participated in this study.

Author Contributions

Chenyi Zhou and Yahao Guo are co-first authors. All authors made a significant contribution to the work reported, whether that is in the conception, study design, execution, acquisition of data, analysis and interpretation, or in all these areas; took part in drafting, revising or critically reviewing the article; gave final approval of the version to be published; have agreed on the journal to which the article has been submitted; and agree to be accountable for all aspects of the work.

Funding

This work was supported in part by grants from Guangdong Provincial Natural Science Foundation (2017A030313841), National Natural Science Foundation Cultivation Project (2021GZRPYM06), Third Affiliated Hospital of Sun Yat-sen University (2023WW605), Suzhou Municipal Science and Technology Bureau (SKYD2023088), and Suzhou Municipal Health Commission (QNXM2024093).

Disclosure

The authors declared no conflict of interest.

References

1. Siegel RL, Miller KD, Jemal A. Cancer statistics, 2020. *Ca Cancer J Clinicians*. 2020;70(1):7–30. doi:10.3322/caac.21590
2. Guo Q, Zhang AL, Xue CC, Coyle ME, Chen Q. A Delphi Study of Expert Consensus on Chinese Medicine Syndrome Differentiation and Herbal Use for Early Breast Cancer, Integr. *Cancer Ther*. 2023;22:153–173. doi:10.1177/15347354231204008
3. Daly GR, Naidoo S, Alabdulrahman M, et al. Screening and Testing for Homologous Recombination Repair Deficiency (HRD) in Breast Cancer: an Overview of the Current Global Landscape, Curr. *Oncol Rep*. 2024;26(8):890–903. doi:10.1007/s11912-024-01560-3
4. Kerlikowske K, Su Y, Sprague BL, et al. Association of Screening With Digital Breast Tomosynthesis vs Digital Mammography With Risk of Interval Invasive and Advanced Breast Cancer. *JAMA-J Am Med Assoc*. 2022;327(22):2220–2230. doi:10.1001/jama.2022.7672
5. Xiao J, Rahbar H, Hippe DS, et al. Dynamic contrast-enhanced breast MRI features correlate with invasive breast cancer angiogenesis. *Npj Breast Cancer*. 2021;7(1):42. doi:10.1038/s41523-021-00247-3
6. Malhaire C, Selhane F, Saint-Martin M, et al. Exploring the added value of pretherapeutic MR descriptors in predicting breast cancer pathologic complete response to neoadjuvant chemotherapy. *Eur Radiol*. 2023;33(11):8142–8154. doi:10.1007/s00330-023-09797-5
7. Li K, Machireddy A, Tudorica A, Moloney B, Huang W. Discrimination of Malignant and Benign Breast Lesions Using Quantitative Multiparametric MRI: a Preliminary Study. *Tomography*. 2020;6(2):148–159. doi:10.18383/j.tom.2019.00028
8. He M, Su J, Ruan H, Song Y, Ma M, Xu F. Nomogram based on quantitative dynamic contrast-enhanced magnetic resonance imaging, apparent diffusion coefficient, and clinicopathological features for early prediction of pathologic complete response in breast cancer patients receiving neoadjuvant chemotherapy, Quant. *Imaging Med Surg*. 2023;13:4089–4102. doi:10.21037/qims-22-869
9. Ramtohul T, Tescher C, Vaflard P, et al. Prospective Evaluation of Ultrafast Breast MRI for Predicting Pathologic Response after Neoadjuvant Therapies. *Radiology*. 2022;305(3):565–574. doi:10.1148/radiol.220389
10. Tsang JYSP, Tse GMF. Molecular Classification of Breast Cancer, Adv. *Anat Pathol*. 2020;27(1):27–35. doi:10.1097/PAP.0000000000000232
11. Ohashi A, Kataoka M, Kanao S, et al. Diagnostic performance of maximum slope: a kinetic parameter obtained from ultrafast dynamic contrast-enhanced magnetic resonance imaging of the breast using k-space weighted image contrast (KWIC). *Eur J Radiol*. 2019;118:285–292. doi:10.1016/j.ejrad.2019.06.012
12. Ohashi A, Kataoka M, A MI, et al. A multiparametric approach to diagnosing breast lesions using diffusion-weighted imaging and ultrafast dynamic contrast-enhanced MRI - ScienceDirect, Magn. *Reson Imaging*. 2020;71:154–160. doi:10.1016/j.mri.2020.04.008
13. Shiau JP, Wu CC, Chang SJ, et al. FAK Regulates VEGFR2 Expression and Promotes Angiogenesis in Triple-Negative Breast Cancer. *Biomedicines*.;9(12):1789. PMID: 34944605; PMCID: PMC8698860. doi:10.3390/biomedicines9121789
14. Luo X, Zou W, Wei Z, et al. Inducing vascular normalization: a promising strategy for immunotherapy, Int. *Immunopharmacol*. 2022;112:109167. doi:10.1016/j.intimp.2022.109167
15. Krüger K, Silwal-Pandit L, Wik E, et al. Baseline microvessel density predicts response to neoadjuvant bevacizumab treatment of locally advanced breast cancer. *Sci Rep*. 2021;11(1):3388. doi:10.1038/s41598-021-81914-0
16. Huang M, Liao B, Xu P, et al. Prediction of Microvascular Invasion in Hepatocellular Carcinoma: preoperative Gd-EOB-DTPA-Dynamic Enhanced MRI and Histopathological Correlation. *Contrast Media Mol Imaging*. 2018;2018(2018):9674565. doi:10.1155/2018/9674565
17. Xu Z, Ding Y, Zhao K, et al. MRI characteristics of breast edema for assessing axillary lymph node burden in early-stage breast cancer: a retrospective bicentric study. *Eur Radiol*. 2022;32(12):8213–8225. doi:10.1007/s00330-022-08896-z

18. Wang X, Venet D, Lifrange F, et al. Spatial transcriptomics reveals substantial heterogeneity in triple-negative breast cancer with potential clinical implications. *Nat Commun*. 2024;15(1):10232. doi:10.1038/s41467-024-54145-w
19. Nagayama Y, Kato Y, Inoue T, et al. Liver fibrosis assessment with multiphasic dual-energy CT: diagnostic performance of iodine uptake parameters. *Eur Radiol*. 2021;31(8):5779–5790. doi:10.1007/s00330-021-07706-2
20. Mireştean CC, Volovăț C, Iancu RI, et al. `. *J Clin Med*. 2022;3(3):616. doi:10.3390/jcm11030616
21. Shapaer T, Chen Y, Pan Y, et al. Elevated BEAN1 expression correlates with poor prognosis, immune evasion, and chemotherapy resistance in rectal adenocarcinoma. *Discover Oncol*. 2024;15(1):446. doi:10.1007/s12672-024-01321-5
22. Yu Y, Chen R, Yi J. Non-invasive prediction of axillary lymph node dissection exemption in breast cancer patients post-neoadjuvant therapy: a radiomics and deep learning analysis on longitudinal DCE-MRI data. *Breast*. 2024;77:10378–10384. doi:10.1016/j.breast.2024.103786
23. Hui L, Mendel KR, Li L, Deepa S, Giger ML. Digital Mammography in Breast Cancer: additive Value of Radiomics of Breast Parenchyma. *Radiology*. 2020;291:15–20.
24. You C, Su G, Zhang X, et al. Multicenter radio-multiomic analysis for predicting breast cancer outcome and unravelling imaging-biological connection. *Npj Precis Oncol*. 2024;8(1):193–205. doi:10.1038/s41698-024-00666-y
25. Wang G, Shi D, Guo Q, Zhang H, Wang S, Ren K. Radiomics Based on Digital Mammography Helps to Identify Mammographic Masses Suspicious for Cancer. *Front Oncol*. 2022;12:843436.
26. Sammut SJ, Crispin-Ortuzar M, Chin SF. Multi-omic machine learning predictor of breast cancer therapy response. *Nature*. 2022;601 (7894):623–629. doi:10.1038/s41586-021-04278-5
27. Naranjo ID, Gibbs P, Reiner JS, et al. Breast Lesion Classification with Multiparametric Breast MRI Using Radiomics and Machine Learning: a Comparison with Radiologists'. *Cancers*. 2022;14(7):1743–1749. doi:10.3390/cancers14071743